2011 50th IEEE Conference on Decision and Control and
European Control Conference (CDC-ECC)
Orlando, FL, USA, December 12-15, 2011

Individualized PID Control of Depth of Anesthesia Based on Patient Model Identification During the Induction Phase of Anesthesia

Kristian Soltesz, Jin-Oh Hahn, *Member IEEE*, Guy A. Dumont, *Fellow IEEE*, J. Mark Ansermino

***Abstract*— This paper proposes a closed-loop propofol admission strategy for depth of hypnosis control in anesthesia. A population-based, robustly tuned controller brings the patient to a desired level of hypnosis. The novelty lies in individualizing the controller once a stable level of hypnosis is reached. This is based on the identified patient parameters and enhances suppression of output disturbances, representing surgical stimuli. The system was evaluated in simulation on models of 44 patients obtained from clinical trials. A large amount of improvement (20 – 30%) in load suppression performance is obtained by the proposed individualized control.**

***Index Terms*— Medical control systems, Drug delivery, Control system synthesis, Medical simulation.**

I. Introduction

During surgical procedures, a combination of anesthetic drugs are given in order to 1) maintain a desired depth of hypnosis (sleep), 2) keep the patient in an analgesic (pain free) state, and in some cases 3) establish a neuro-muscular blockade to avoid movement. This paper focuses on the problem of individualized closed-loop control of depth of hypnosis (DOH) based on propofol administration. Fig. 1 outlines the system from a control engineering point of view.

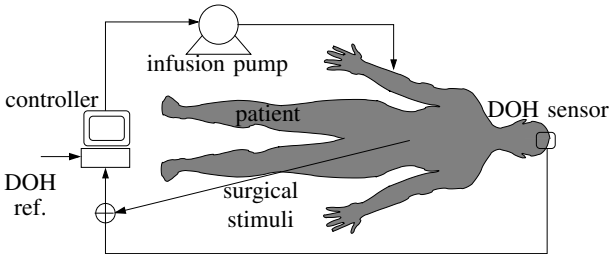

Fig. 1. Closed-loop DOH control system.

Propofol hypnosis can be divided into three temporal phases. During the *induction* phase, the aim is to bring the patient to a reference DOH level. Once a stable DOH close to the reference is achieved, the *maintenance* phase, during which surgery takes place, begins. The surgical stimuli can be viewed as output disturbances, reducing the DOH. At the same time, the administration of analgesic drugs increase the DOH via anesthetic-opioid synergy. Hence, the challenge during the maintenance phase is to administer propofol to counteract the disturbances, without over- or under-dosing. Once surgery is completed, the *emergence* phase, during which administration of propofol is terminated, takes place.

The aim of this paper is to examine the potential benefit of individualized propofol delivery based on controller retuning at the end of the induction phase. The main advantage of a single update before the maintenance phase begins, as opposed to continuous adaptation (see e.g. [1]), is that unmeasured disturbances during the maintenance phase do not result in poor performance or even instability due to drifting parameters. Focus does not lie on the controller tuning per se, but rather on what can be gained by the proposed individualization. The rationale supporting this papar can therefore be combined with previous work in the area of closed-loop propofol anesthesia, such as [2], [3] and [4].

The paper is organized as follows: Section II presents the models that controller synthesis is based upon. The PID controller and its tuning is explained in Section III. Patient model parameter identification for individualized control is the topic of Section IV. The proposed control scheme is evaluated in a simulator, explained in Section V. Simulation results are presented and discussed in Section VI. Finally, conclusions are drawn in Section VII.

II. Model of the Propofol-DOH Process

Patient models for anesthesia consist of a pharmacokinetic (PK) model explaining the distribution and metabolism of the drug, and a pharmacodynamic model relating the plasma drug concentration to clinician effect. In a previous work [5] PK and PD parameters were derived from demographic data, based on which robust controllers were synthesized to handle inter- and intra-patient variability.

Controller and PD identifier were designed based on the patient PKPD model with the propofol infusion rate u as input and the DOH measurement y as output.

A. Parameters and Signals

Table I lists signals and parameters used throughout the paper.

B. Pharmacokinetic (PK) Model

The PK model relates infusion rate u to plasma concentration C_p. In this paper, the Schüttler PK model [6] was used. It is a three-compartment mamillary model, outlined in Fig. 2. Each compartment represents a class of tissues.

Kristian Soltesz is with the Department of Automatic Control, Lund University, Lund Sweden kristian@control.lth.se

Jin-Oh Hahn is with the Department of Mechanical Engineering, University of Alberta, Edmonton, Canada jinoh.hahn@ualberta.ca

Guy A. Dumont is with the Department of Electrical and Computer Engineering, University of British Columbia, Vancouver, Canada guyd@ece.ubc.ca

J. Mark Ansermino is with the Department of Anesthesiology Pharmacology and Therapeutics, University of British Columbia, Vancouver, Canada anserminos@yahoo.ca

symbol	unit/range	name
$\mathbf{A}$, $\mathbf{B}$, $\mathbf{C}$	-	Schüttler PK system matrices
C_e	mg·l^{-1}	Effect site concentration
C_p	mg·l^{-1}	Primary compartment concentration
C_{p_m}	mg·l^{-1}	Estimate of C_p from E_m
DOH	(100,0)	Depth of hypnosis (100 $\Leftrightarrow$ awake)
e_L	-	Load step control error
E	(0,1)	Normalized DOH (0 $\Leftrightarrow$ awake)
E_m	(0,1)	Estimate of E from y
E_{m_σ}	-	Signal threshold
EC_{50}	mg·l^{-1}	Hill gain parameter
h	s	Controller sample period
$k_{ij} i,j=1,2,3$	s^{-1}	Rate constants (flow $i \to j$)
k_d^{-1}	s	Effect PD time constant
k_{10}	s^{-1}	Elimination rate constant
K	-	True FOTD gain
$\hat{K}$	-	Estimate of K
K_D	-	Derivative controller gain
K_I	-	Integral controller gain
K_P	-	Proportional controller gain
L	-	True FOTD delay
$\hat{L}$	-	Estimate of L
N	-	Maximal derivative gain
$p_k,\ k=1,2,3$	-	Schüttler PK poles
r	(0,1)	Normalized DOH reference
t_γ	s	Duration of γ identification
t_{ind}	s	Duration of induction phase
T	-	True FOTD time constant
$\hat{T}$	-	Estimate of T
T_d	s	Effect PD delay
T_I	s	Controller integral time
T_D	s	Controller derivative time
T_r	s	Reference filter time constant
T_t	s	Anti-windup tracking time
u	mg·s^{-1}	Infusion rate
$u_{\max}$	mg·s^{-1}	Upper bound of control signal
$u_{\min}$	mg·s^{-1}	Lower bound of control signal
u_σ	-	Signal threshold
v	-	Signal in Hill function
$\hat{v}$	-	Feedback quantity
v_m	-	Estimate of v from E
V_1	l	Primary compartment volume
$\mathbf{x}=[x_1\ x_2\ x_3]^T$	mg·l^{-1}	Compartment concentrations
x_D	-	PID derivative filter state
x_I	-	PID integrator state
y	(0,1)	Normalized measured DOH
γ	-	Hill slope parameter
$\hat{\gamma}$	-	Estimate of γ

TABLE I

SIGNALS AND PARAMETERS.

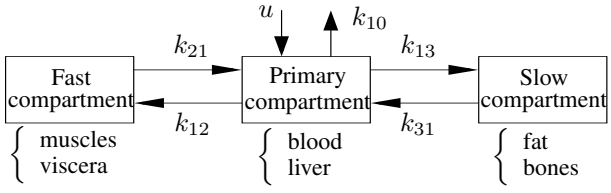

Fig. 2. Schüttler's three-compartment mammillary model.

The drug is delivered into the primary (central) compartment with rate u. Denoting $\mathbf{x}$ the vector of drug concentration in each compartment, the Schüttler's model is given by

$$\dot{\mathbf{x}} = \begin{bmatrix} -(k_{10}+k_{12}+k_{13}) & k_{12} & k_{13} \\ k_{21} & -k_{21} & 0 \\ k_{31} & 0 & -k_{31} \end{bmatrix} \mathbf{x} + \frac{1}{V_1} \begin{bmatrix} 1 \\ 0 \\ 0 \end{bmatrix} u. \tag{1}$$

The transfer function representation of (1) from u to x_1 is

$$G_{C_p,u}(s) = \frac{1}{V_1} \frac{(s+k_{21})(s+k_{31})}{(s+p_1)(s+p_2)(s+p_3)}, \tag{2}$$

where $p_k,\ k \in \{1,2,3\}$ are defined accordingly from k_{ij}. It was concluded by Schüttler et al. [6] that *age* and *lean body mass* are reliable demographic covariates for the parameters of (2). Functions relating these covariates to volumes and clearance rates $V_1, k_k,\ k \in \{1,2,3\}$ are presented in [6].

C. Pharmacodynamic (PD) Model – Hill Function

1) Effect Site Dynamics: The output of the Schüttler PK model is the primary compartment concentration of propofol, C_p. However, the effect site of the drug is the brain, not the plasma. To account for the distribution of drug from the plasma to the effect site, the PK model was augmented by a delayed first order system [7]:

$$G_{C_e,C_p}(s) = \frac{k_d}{s+k_d} e^{-T_d s}, \tag{3}$$

where the delay is intended to model the drug transport from the intravenous to the effect site.

2) Dose-Response Characteristics: The clinical effect E is normalized to $(0,1)$, where 0 corresponds to fully awake state. In the steady state, the relation between C_e and E is well described by a sigmoidal $E_{\max}$ function:

$$E(C_e) = \frac{C_e^\gamma}{EC_{50}^\gamma + C_e^\gamma}, \tag{4}$$

which is also known as the Hill function. It is parametrized by EC_{50}, the value of C_e corresponding to $E = 0.5$, and γ, defining the steepness of the sigmoidal curve. The Hill function (4) can be decomposed into a series of a linear gain

$$v(C_e) = \frac{1}{2EC_{50}} C_e, \tag{5}$$

and a sigmoidal nonlinearity

$$E = f(v;\gamma) = \frac{v^\gamma}{\frac{1}{2}^\gamma + v^\gamma}, \tag{6}$$

which is parametrized only in γ. It is obvious from (6) that $E = 0.5$ corresponds to $v = 0.5$.

For model identification purposes, the effect PD and linear Hill gain are lumped together to yield the following first order time delayed (FOTD) system:

$$v(s) = \frac{K_d/(2EC_{50})}{s+K_d} e^{-sT_d} C_p(s), \tag{7}$$

whereas the nonlinear part (6) is treated separately.

D. Clinical Front End

There are several clinical options for measuring DOH based on the electroencephalogram (EEG), which can be sampled using non-invasive probes mounted on the patient's forehead. The most popular option is the Bispectral Index (BIS) [8], for which commercial instrumentation equipment are available. However, BIS is not ideal for control design purposes since its dynamics are strongly time-varying and that the proprietary algorithm often exhibits nonlinear behavior. The use of wavelet techniques has been proposed to overcome these challenges, yielding the WAV_{CNS} index [9]. It correlates well with BIS, and moreover, it has time-invariant linear dynamics:

$$G_{y,E}(s) = \frac{1}{(8s+1)^2}, \tag{8}$$

which is preferable to BIS from a control design perspective. The WAV_{CNS} monitor is graded in BIS units. They range $(0, 100)$, where 100 corresponds to the fully awake state.

E. PKPD Model

The patient model is obtained by combining the PK and PD models. A block diagram of this combination, together with the WAV_{CNS} monitor, is shown in Fig. 3.

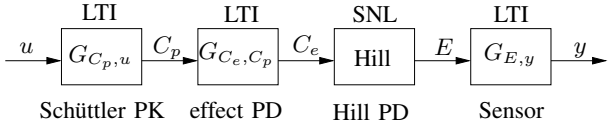

Fig. 3. PKPD patient and sensor model, relating DOH y to propofol infusion rate u. Subsystems are linear time invariant (LTI) or static nonlinearities (SNL).

It was demonstrated that PK parameters of propofol are linear in the range $25 - 200$ $\mu\text{g}\cdot\text{kg}^{-1}\cdot\text{min}^{-1}$ and that the model is generally invalid outside this range [10]. Similarly, the Hill function (4) describes the steady-state relation between C_e and E.

F. Surgical Stimuli

Surgical stimulation was modeled as an output disturbance, which was adapted from [4] (see Fig. 4).

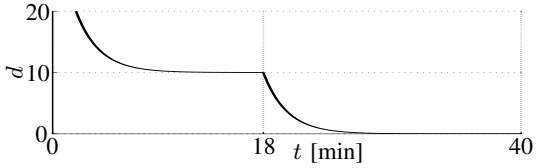

Fig. 4. Disturbance profile from [4].

III. Robust PID Control Synthesis

A two-degrees-of-freedom PID controller was designed for DOH control. Two novel output filters were introduced in this paper in an effort to facilitate control design by effectively cancelling out the monitor dynamics and the Hill function nonlinearity.

A. Output Filter I

The system shown in Fig. 3 cannot be readily divided into its LTI and static nonlinearity components, due to the existence of the Hill function between the effect PD and the monitor dynamics. This is a limiting factor in both patient model identification and controller synthesis. To overcome this problem, we propose to augment a delayed inverse of the monitor dynamics as follows. The control system operates at 1 Hz. A zero order hold (ZOH) sampling of (8) with period $h = 1$ s yields

$$G^h_{y,E}(z) = \frac{1}{100}\frac{0.719z + 0.662}{z^2 - 1.765z + 0.778}. \tag{9}$$

To invert (9) without introducing acausality, a delay of h was added, resulting in the delayed inverse:

$$F_1(z) = 100\frac{z^2 - 1.765z + 0.778}{0.719z^2 + 0.662z}. \tag{10}$$

This filter was applied to the sensor output to convert the system dynamics to a standard Wiener model by canceling out the effect of the monitor dynamics. The sensor plus the delayed inverse was modeled as a delay h in controller synthesis. Depending on the high pass nature of the drug delivery actuator, further filtering might therefore be desirable.

B. Output Filter II

The model in Fig. 3 is nonlinear due to the Hill function. In the context of synthesizing a maintenance phase controller, this can be approached by linearizing (4) around the operating point $C_e = EC_{50}$. However, this is not acceptable during the induction phase, in which no well-defined operating point exists. If a PID controller (or any controller involving integral action) is used, the integral state will build up rapidly during the beginning of the induction phase due to the low dose concentrations, $C_p \ll EC_{50}$. This will in turn cause an undershoot of the WAV_{CNS} response. A possible remedy to alleviate this problem is to reduce the integral action, but this may increase the duration of the induction phase. To facilitate the controller design by further linearizing the system dynamics, an additional linearizing filter was used in series with (10) as follows. The inverse of the non-linear part of the Hill function (6) is given by

$$v = F_2(E;\gamma) = f^{-1}(E;\gamma) = \frac{1}{2}\left(\frac{E}{1-E}\right)^{\frac{1}{\gamma}}. \tag{11}$$

Letting γ and $\hat{\gamma}$ be the true and demographics-based slope parameters, respectively, yields

$$\hat{v} = f^{-1}(f(v;\gamma);\hat{\gamma}) = \frac{1}{2}(2v)^{\gamma/\hat{\gamma}}, \tag{12}$$

which is close to v when $\hat{\gamma} \approx \gamma$. The controller was based on the assumption that $\hat{\gamma} = \gamma$ and that the nonlinearity was completely cancelled out by closing the loop from $\hat{v}$ in (12).

C. Plant Model

Combining (2), (3), (5), (9), (10) and (12) and assuming $\hat{\gamma} = \gamma$ yields the plant model

$$P(s) = \frac{k_d}{2EC_{50}V_1} \frac{(s+k_{21})(s+k_{31})e^{-s(T_d+h)}}{(s+p_1)(s+p_2)(s+p_3)(s+k_d)}, \quad (13)$$

which was used for controller synthesis.

D. Controller

The PID controller was parametrized in its proportional (K_p), integral (K_I) and derivative (K_D) gains. Two robust PID design methods, outlined below, were evaluated to determine these gains. They are both based on minimizing norms of the tracking error caused by step load disturbances.

1) Robust Load IE Minimization: The objective of this method is to find PID parameters $\{K_P, K_I, K_D\}$ that minimize the integral of the control error (IE) e_L caused by a step load disturbance. Robustness is enforced by restricting the open-loop Nyquist curve outside a circular disc with radius M_s, centered at -1. This is equivalent to restricting the ∞-norm of the sensitivity function:.

$$\min_{K_P,K_I,K_D} \int_0^\infty e_L(\tau)d\tau, \quad (14)$$

$$s.t. \max_\omega |S(\omega)| \leq M_s. \quad (15)$$

See [11] for a thorough description of the method or [12] for a summary. A regimen for determining suitable M_s is described in [4].

2) Robust Load IAE Minimization: An oscillatory zero-mean error can yield small IE values, yet is not desirable. This can be prevented by using the following optimization constraint:

$$\min_{K_P,K_I,K_D} \int_0^\infty |e_L(\tau)|d\tau. \quad (16)$$

The minimized quantity is referred to as the integral absolute error (IAE). A useful algorithm is presented in [13].

E. Reference Filter

In order to avoid oscillations and over-dosing during the induction phase, the reference was processed using the following filter, whose time constant T_r was chosen according to [14].

$$F_r(s) = \frac{1}{sT_r + 1}. \quad (17)$$

F. Implementation Aspects

1) Saturation and Integrator Anti-Windup: The control signal has a natural lower bound $u_{\min} = 0$ (since drug cannot be extracted once infused). For safety reasons, an upper bound $u_{\max}$ of 3.33 mg·s^{-1} was also introduced. Tracking was utilized in order to avoid integral windup; see Fig. 5(b). The tracking constant was heuristically chosen as the geometric mean of the PID integral ($T_I = \frac{K_P}{K_I}$) and derivative ($T_D = \frac{K_D}{K_P}$) times as suggested in [12]:

$$T_t = \sqrt{T_I T_D} = \sqrt{\frac{K_D}{K_I}}. \quad (18)$$

2) Setpoint Weighting: In this paper, disturbance rejection and absence of output oscillations are prioritized to tight reference tracking. Hence, a zero setpoint weight was chosen for proportional and derivative components of the controller, forcing the reference to enter the control signal only through the integral term, as shown in Fig. 5(b).

3) Derivative Filter: To suppress the high frequency noise, the differentiator $K_D s$ was filtered as

$$\frac{sK_P K_D N}{sK_D + K_P N}, \quad (19)$$

where $N = 5$ was chosen heuristically to yield an adequate trade off between noise suppression and phase lead. Note that the reference was not differentiated to facilitate a smooth response to rapid and abrupt reference changes.

4) Derivative Kick: The low-pass reference filter combined with the zero setpoint weight resulted in a slow increase of u, and consequently y, during the beginning of the induction phase, which is not desirable, since the propofol infusion is painful to the patient while the DOH is low. To avoid this problem, the derivative term of the PID control signal was set to a strictly positive value during the beginning of the induction phase, yielding a spike in u.

5) Discretization: The controller was discretized using the approximation $s \approx z - 1$, which is acceptable since the sample period is small compared to the dominant time scale of the system. Using ZOH discretization or performing the tuning optimization in the discrete time domain would have been other options. However, they lack the intuitive insight provided by the continuous-time PID control architecture that the proposed discretization preserves.

6) Bumpless Parameter Changes: Let x_I and x_D be the state of the PID integrator and derivative filter, shown in Fig. 5(b) and Fig. 5(c). The control signal is given by

$$u = \text{sat}_{u_{\min}}^{u_{\max}}(\underbrace{-\hat{v}K_P}_{P} + \underbrace{x_I}_{I} \underbrace{-\hat{v}K_P N - x_D \frac{K_P N}{K_D}}_{D}). \quad (20)$$

Switching the set of PID controller parameters from $\{K_P, K_I, K_D\}$ to $\{K'_P, K'_I, K'_D\}$ at the end of the induction phase, may lead to discontinuity in the derivative term, resulting in discontinuity in the control signal. This risk was prevented by simultaneously updating the states as follows:

$$x'_D = \hat{v}(K'_P - K_P)\frac{K'_D}{K'_P} - x_D \frac{K_P}{K_D}\frac{K'_D}{K'_P}, \quad (21)$$

$$x'_I = x_I + \hat{v}(K'_P - K_P). \quad (22)$$

G. Closed-Loop System

Summarizing, Fig. 5(a) shows the block diagram of the closed loop system, including patient, controller and filters, discussed above. The block diagram of the PID controller is shown in Fig. 5(b). The derivative filter block of Fig. 5(b) is illustrated in detail in Fig. 5(c).

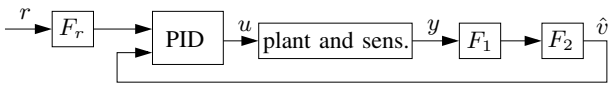

(a) Closed-loop system. The plant and sensor is equivalent to Fig. 3.

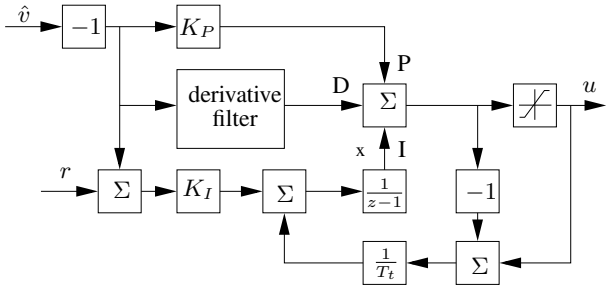

(b) PID controller. The derivative filter block contains the ZOH discretization of (19).

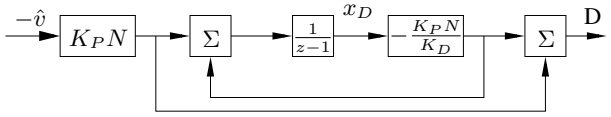

(c) The derivative filter (19) block of Fig. 5(b).

Fig. 5. Closed-loop system and PID controller.

IV. System Identification

The objective of the system identification was to derive parameter estimates for the model that relates C_p to E; see Fig. 3. The model consists of the FOTD (7), parametrized in

$$K = \frac{1}{2EC_{50}},\ T = \frac{1}{K_d},\ L = T_d, \tag{23}$$

and the nonlinear part of the Hill function (6), parametrized in γ. Since E is not directly available, its estimate E_m was used. It was obtained by applying F_1 in (10) to y. Likewise, an estimate C_{p_m} of C_p, obtained by driving the PK model (2) with u, was used.

A. Hill Function Nonlinearity

Since v in (7) ranges from 0 to ≈ 0.5 during the induction phase, linearizing (7) around a nominal value does not present a feasible approach towards PD model parameter identification. Furthermore, it is not trivial to simultaneously identify the LTI parameters $\{K, T, L\}$ and the Hill function parameter γ. For this reason a two-stage approach was employed. The parameter γ was identified and fixed during the first stage and LTI parameters were identified during the second stage.

B. Initial Parameter Estimates

Inspecting the simulation pairs of u and E reveals that the first order dynamics are fast compared with the time scale of induction. Hence, it was reasonable to approximate (7) by a delayed gain $K \cdot e^{-Ls}$.

The initial estimate $\hat{L}$ of L was obtained by identifying the time instants after which E_m and u stay above thresholds E_{m_σ} and u_σ, respectively. The initial estimate $\hat{K}$ of K was then obtained by averaging the ratio of E_m and u over the last 3 min of the induction phase.

Subsequently, the initial estimate $\hat{\gamma}$ of γ was obtained by a bisection search, which minimized (the discretized equivalent of)

$$\int_0^{t_\gamma} \left(f^{-1}(E_m;\hat{\gamma})(t) - KC_{p_m}(t+L)\right)^2 dt. \tag{24}$$

Fixing $\hat{\gamma}$ yielded the estimate v_m of v:

$$v_m = f^{-1}(E_m;\hat{\gamma}). \tag{25}$$

Finally, a bisection search was used to find the estimate $\hat{T}$ of T, which minimized (the discretized equivalent of)

$$\int_0^{t_{\text{ind}}} \left(v_m(t) - \mathcal{L}^{-1}\left(\frac{\hat{K}e^{-s\hat{L}}}{s\hat{T}+1}C_{p_m}\right)\right)^2 dt. \tag{26}$$

C. PD Identification Using Induction Phase Response

A gradient-based identification method [15] was employed to obtain refined estimates of the PD model parameters from the patient's response during the induction phase. The parameter estimates were identified to minimize

$$J(\hat{\theta}) = \int_0^{t_{\text{ind}}} (v_m - \hat{v})^2 dt, \tag{27}$$

where v_m was parametrized in $\hat{\theta} = \{K, T, L\}$ (while $\hat{\gamma}$ was fixed). Computing the gradient $\nabla J(\hat{\theta})$ was done by simulating an augmented system, where the augmented states were partial derivatives of the objective function (27) with respect to the PD model parameters to be identified. Details of the methods are outlined in [15].

V. Simulated Experiment

The surgical procedure was simulated for each patient in the test population, as described below.

A. Test Population

The test population consisted of 44 PKPD models. Model parameters were derived using clinical data and are disclosed in [4]. In the course of PD identification, it was assumed that individual PK models can be accurately characterized using Shcüttler's covariate formulae [6]. This essentially lumps all the parametric uncertainty into the PD model.

B. Experiment Layout

1) Induction Phase: Prior to the simulated surgical procedure, the induction phase controller was synthesized according to Section III, based on the control design model (13). Parameters k_{21}, k_{31}, p_1, p_2 and p_3 were computed from the patient age and weight using Schüttler's formulae, while population averages were used for K_d, EC_{50} and T_d. Propofol was administered using this population-based controller during the induction phase of the simulated surgical procedure.

2) PD Identification and Controller Re-Design: PD parameters were estimated as described in Section IV. At the end of the induction phase, the estimated PD parameters were used to synthesize an individualized controller, based on the same procedure as the induction phase controller.

3) Maintenance and Emergence Phases: During the beginning of the maintenance phase, the simulation state was saved to allow for parallel maintenance phase simulations with (i) the induction phase controller, (ii) the individualized controller and (iii) and an ideal controller based on the actual parameter values of the simulated patient. Signals from these simulations were saved and analyzed as described in Section VI.

C. PK Uncertainty

In order to introduce a realistic amount of PK uncertainty in the simulated procedure, perturbations were given to the parameters of the patient model. This was done using normally distributed random numbers with standard deviations chosen as the standard deviations of the prediction residuals reported in Schüttler et al. [6]. Nominal values were used for the controller synthesis.

VI. Results and Discussion

Overall, the individualized controller outperformed the population-based controller. Fig. 6 shows the simulation profiles for each of the 44 patients, using the individualized controller. In terms of IAE, the individualized controller could provide a 23 % reduction in error over the 44 patient models, compared with the population-based controller. Moreover, it was only 4 % larger than with the ideal controller, synthesized using the true patient PKPD models. The results clearly demonstrate the potential of an individualized control scheme.

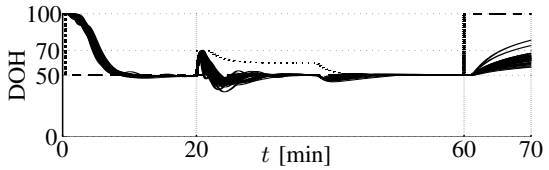

(a) Measured DOH with disturbance profile of Fig. 4.

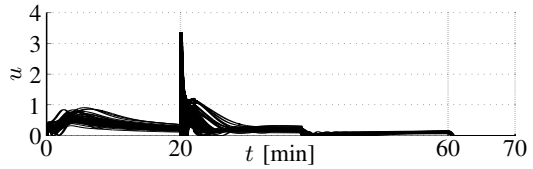

(b) Infusion profiles with disturbance profile of Fig. 4.

Fig. 6. Measured DOH and infusion profiles of the test population.

The use of an output filter (11) significantly improved the reference tracking performance in the induction phase. In the absence of the filter, undershoots by as much as 30 BIS units were observed in some patients.

Due to the presence of the perturbations in the PK models, the identified PD parameters generally did not converge to the patient values. Instead they converged to values close to their true counterparts in order to compensate for the PK mismatch. It should be noted, however, that the identified PD parameters converged to the true parameter values when the PK model uncertainty was not considered.

Although rigorous parameter convergence proof is not feasible due to the non-convexity of the system identification problem discussed in Section IV, the proposed two-stage identification strategy was able to provide accurate parameter estimates for all the simulated procedures. In a future study, however, its validity and performance needs to be extensively examined before it can be introduced into clinical practice.

VII. Conclusion

A novel propofol administration strategy for closed-loop DOH control has been proposed. Evaluation of the proposed control scheme in simulated procedures over wide-ranging PKPD models with parameter perturbations suggested that 1) the closed-loop performance can be significantly enhanced by employing the individualized controller based on the PD model identified using the induction phase response, and that 2) the proposed control scheme is equipped with a sufficient level of robustness against uncertainty in the PK model.

References

[1] W. M. Haddad, T. Hayakawa, and J. M. Bailey, "Adaptive control for nonlinear compartmental dynamical systems with applications to clinical pharmacology," *System & Control Letters*, vol. 55, no. 1, pp. 62 –70, 2006.

[2] A. Gentilini, M. Rossoni-Gerosa, C. W. Frei, R. Wymann, M. Morari, A. M. Zbinden, and T. W. Schnider, "Modeling and closed-loop control of hypnosis by means of bispectral index (BIS) with isoflurane," *IEEE Transactions on Biomedical Engineering*, vol. 48, no. 8, pp. 874 – 889, 2001.

[3] C. M. Ionescu, R. D. Keyser, B. C. Torrico, T. D. Smet, M. M. R. F. Struys, and J. E. Normey-Rico, "Robust predictive control strategy applied for propofol dosing using bis as a controlled variable during anesthesia," *IEEE Transactions on Biomedical Engineering*, vol. 55, no. 9, pp. 2161 –2170, 2008.

[4] G. A. Dumont, A. Martinez, and M. Ansermino, "Robust control of depth of anesthesia," *International Journal of Adaptive Control and Signal Processing*, vol. 23, no. 5, pp. 435 – 454, 2009.

[5] S. Bibian, C. R. Ries, M. Huzmezan, and G. Dumont, "Introduction to automated drug delivery in clinical anesthesia," *European Journal of Control*, vol. 11, no. 6, pp. 535 – 537, September 2005.

[6] J. Schüttler and H. Ihmsen, "Population pharmacokinetics of propofol: A multicenter study," *Anesthesiology*, vol. 92, no. 3, pp. 727–738, March 2000.

[7] S. Bibian, "Automation in clinical anesthesia," Ph.D. dissertation, University of British Columbia, Department of Electrical and Computer Engineering, July 2006.

[8] J. W. Johansen and P. S. Sebel, "Development and clinical application of electroencephalographic bispectrum monitoring," *Anesthesiology*, vol. 93, no. 5, pp. 1336 – 1344, November 2000.

[9] T. Zikov, S. Bibian, G. Dumont, M. Huzmezan, and C. Ries, "Quantifying cortical activity during general anesthesia using wavelet analysis," *IEEE Transactions on Biomedical Engineering*, vol. 53, no. 4, pp. 617 – 632, April 2006.

[10] T. W. Schnider, C. F. Minto, P. L. Gambus, C. Andresen, D. B. Goodale, S. L. Shafer, and E. J. Youngs, "The influence of method of administraion and covariates on the pharmacokinetics of propofol in adult volunteers," *Anesthesiology*, vol. 88, no. 5, pp. 1170 – 1182, May 1998.

[11] H. Panagopoulos, K. J. Åström, and T. Hägglund, "Design of PID controllers based on constrained optimisation," *IEE Proceedings - Control Theory & Applications*, vol. 149, no. 1, pp. 32–40, 2002.

[12] K. J. Åström and T. Hägglund, *Advanced PID Control*. ISA, 2006.

[13] O. Garpinger and T. Hägglund, "A software tool for robust PID design," in *Proc. 17th IFAC World Congress, Seoul, Korea*, July 2008.

[14] A. Martinez, "Robust control: Pid vs fractional control design, a case study," Master's thesis, University of British Columbia, Canada, November 2005.

[15] K. Soltesz, T. Hägglund, and K. J. Åström, "Transfer function parameter identification by modified relay feedback," in *Proc. American Control Conference, Baltimore, USA*, January 2010.